

Spin-Charge Separation in Two-dimensional Frustrated Quantum Magnets

Andreas Läuchli and Didier Poilblanc
*Laboratoire de Physique Théorique, CNRS-UMR 5152,
 Université Paul Sabatier, F-31062 Toulouse, France*
 (Dated: June 16, 2004)

The dynamics of a mobile hole in two-dimensional frustrated quantum magnets is investigated by exact diagonalization techniques. Our results provide evidence for spin-charge separation upon doping the *kagomé* lattice, a prototype of a spin liquid. In contrast, in the checkerboard lattice, a symmetry broken Valence Bond Crystal, a small quasi-particle peak is seen for some crystal momenta, a finding interpreted as a restoration of weak holon-spinon confinement.

PACS numbers: 71.10.Hf, 71.20.-b

In the last years, there has been growing interest in the investigation of frustrated magnets, both on experimental and theoretical sides. Spin-1/2 Heisenberg models on two and three dimensional (3D) lattices have been studied extensively providing increasing evidences for new exotic phases like the spin liquid Resonating Valence Bond (RVB) [1] state or the Valence Bond Crystal (VBC) [2]. In two dimension (2D), the checkerboard lattice [3, 4, 5], i.e. the 2D analog of the 3D pyrochlore lattice, and the *kagomé* lattice [6, 7] (see Fig. 1), respectively, seem to provide simple theoretical realizations of VBC and RVB groundstates (GS). In addition, an exotic scenario where magnons break up into ($S = 1/2$) deconfined spinons [8] could take place in a RVB state. These theoretical conjectures have triggered a renewal of experimental activity on quantum frustrated magnets like e.g. the ($S = 3/2$) *kagomé* compound $\text{SrCr}_9\text{Ga}_{12-9p}\text{O}_{19}$ [9] and the pyrochlore titanates $\text{RE}_2\text{Ti}_2\text{O}_7$ (where RE is a rare-earth magnetic atom such as gadolinium or terbium) [10]. These materials exhibit very rich phase diagrams as a function of chemical composition, temperature, pressure and magnetic field which underline the crucial role of geometric frustration. Furthermore, the recent discovery of superconductivity in a CoO_2 based compound with triangular layers [11] has revived interest in exotic RVB mechanisms of superconductivity [12].

In this Letter, we investigate the dynamics of a mobile hole injected in various 2D frustrated quantum magnets. This study is indirectly motivated by the long-standing puzzles offered by the “normal phase” of high- T_c superconductors whose discovery initiated a search for spin-charge separation mechanisms in 2D and the first proposal of 2D Luttinger liquids [13]. The dynamics of a mobile hole doped into an (Ising) antiferromagnet (AF) was first studied by Brinkman and Rice [14] and a coherent motion was later predicted by Trugman [15]. However, a close inspection of the hole spectral function showed evidences for a composite nature of the doped hole quasi-particle (QP) showing holon and spinon components [16]. Large quantum fluctuations present in frustrated magnets might then induce a complete deconfinement of the hole components. Here we present large scale exact diag-

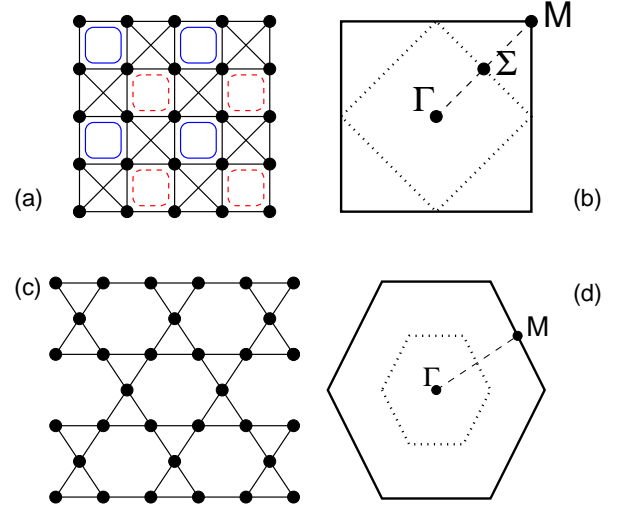


FIG. 1: (a) Schematic picture of the VBC GS of the Heisenberg model on the checkerboard lattice. The two degenerate singlet patterns are shown with full blue and dashed red lines. (b) Dotted line: Brillouin zone (BZ) of the checkerboard lattice. Full line: extended BZ equivalent to the square lattice BZ. The path from the zone center Γ to the $\mathbf{k} = (\pi, \pi)$ point M is shown as a dashed line. (c) The *kagomé* lattice; (d) Dotted line: BZ of the *kagomé* lattice. Full line: extended BZ equivalent to the nondepleted triangular lattice BZ.

onalization results for single hole spectral functions and hole-spin correlations obtained on the checkerboard and the *kagomé* antiferromagnets. A finite lifetime of the hole (breaking apart into a spin 1/2 spinon and a charge $Q = e$ holon) is signaled by the absence of a QP peak in the computed spectral functions. Since the latter could, in principle, be measured by Angular Resolved Photoemission Spectroscopy (ARPES) on high-quality (cleaved) *insulating* single crystals [17], our results can provide motivation and theoretical background to experimentalists. In addition, this investigation might also be relevant to lightly doped samples. Evidences for spin-charge separation in the *kagomé* spin liquid GS are provided while, in the checkerboard lattice, we find small QP peaks for some momenta.

Before going further, let us first summarize briefly the properties of the undoped insulating systems we are dealing with. The checkerboard lattice is believed to form a VBC with plaquette singlets on a subset of the void plaquettes [3, 4, 18, 19]. The groundstate manifold is two fold degenerate [see Fig. 1 (a)]. The system has quite a sizable triplet gap $\Delta_T \approx 0.7J$ [4, 5], and a somewhat smaller singlet gap $\Delta_S \approx 0.3J$ [4, 19] to domain wall like singlet excitations [19]. Based on this picture of a fully gapped system, we expect a coherent QP motion of an injected hole at least in parts of the Brillouin zone (BZ) as observed for example in Heisenberg ladders or dimerized spin chains. On the other hand, the undoped *kagomé* lattice has a very interesting and puzzling groundstate of a new type: while this system is also magnetically disordered [6], it has quite a small triplet gap ($\Delta_T \approx 0.05J$) [7]. The singlet sector seems to remain gapless showing an exponentially large number of singlets within the spin gap [7, 20]. These unconventional low lying excitations open the door to new and surprising phenomena upon hole doping.

Our numerical calculations are based on the standard t - J model Hamiltonian:

$$-t \sum_{\langle i,j \rangle, \sigma} \mathcal{P} \left(c_{i,\sigma}^\dagger c_{j,\sigma} + \text{h.c.} \right) \mathcal{P} + J \sum_{\langle i,j \rangle} \mathbf{S}_i \cdot \mathbf{S}_j - \frac{1}{4} n_i n_j \quad (1)$$

where on both lattices all bonds have the same couplings t and J . This model is believed to be reliable to describe weakly doped Mott-Hubbard insulators with large optical gaps. Hereafter, a physical value of $J/|t| = 0.4$ is assumed, unless mentioned otherwise. The spectral functions are defined in the standard way:

$$A^\sigma(\mathbf{k}, \omega) = -\frac{1}{\pi} \text{Im} \left[\langle \Psi_0 | c_{\mathbf{k},\sigma}^\dagger \frac{1}{\omega + E_0 + i\eta - H} c_{\mathbf{k},\sigma} | \Psi_0 \rangle \right], \quad (2)$$

and calculated by the Lanczos continued-fraction technique on finite clusters of up to 32 sites with periodic boundary conditions. Here $|\Psi_0\rangle$ (of energy E_0) is the GS of the undoped insulating system, so that the dynamics of a *single* hole is probed. A simple sum rule is satisfied: $\int A^\sigma(\mathbf{k}, \omega) d\omega = N_\sigma / N \simeq 1/2$, independent of \mathbf{k} . Therefore the spectral function plots share an arbitrary, but common scale, unless mentioned otherwise. In addition an artificial broadening $\eta = 0.05|t|$ or $0.1|t|$ has been used to plot the data. The weights of the lowest peaks can be obtained exactly, independent of η . We have indicated this weight in the plots when a QP peak is present.

As a first step it is of special interest to consider the static limit i.e. the case $t = 0$ (equivalent to an infinite hole mass) where a spin 1/2 is replaced by an inert (impurity-like) site. The spectral function, which becomes here independent of momentum \mathbf{k} , gives useful hints on the host magnetic disturbance induced by the static hole. Results in Fig. 2 show very different qualitative behaviors for the checkerboard and the *kagomé*

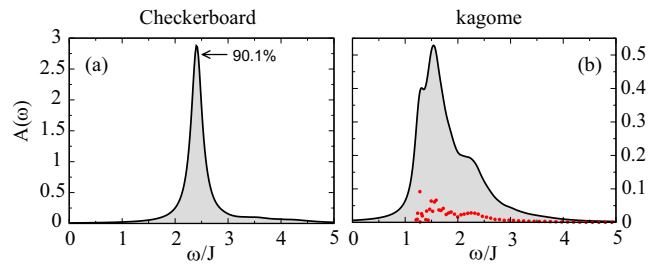


FIG. 2: Single hole spectral function for a static ($t = 0$) hole in a checkerboard (a) or a *kagomé* (b) lattice. The checkerboard spectral function is dominated by the lowest energy peak, in contrast to the *kagomé* response. For this case the weight of the poles is indicated by red circles.

lattices. A sharp peak which exhausts most of the spectral weight is found in the checkerboard lattice. This is consistent with the picture of breaking a local plaquette singlet, therefore producing a localized moment, which remains confined to the hole. The very large peak weight shows that the bare state $c_{i,\sigma} |\Psi_0\rangle$ is a very good approximation of the true one hole groundstate. This however seems to be quite different for the *kagomé* case: the spectral function shows a rather broad response, with no pronounced low energy peak [see weight distribution (circles) in Fig. 2 (b)]. Here the overlap of the bare electron removal state and the true groundstate of the one impurity problem is tiny. This can be nicely understood in the “dimer freezing” picture advocated in Ref. [21], where the screening of the impurity constitutes an important deformation of the RVB spin liquid groundstate. This suggests that a single dopant in the *kagomé* lattice generates a dimer-screened holon with charge $Q=e$ and spin $S=0$ and a deconfined spinon ($Q=0$, $S=1/2$).

We now move to the case of a dynamic hole ($t \neq 0$). Because of the absence of particle-hole symmetry in frustrated lattices one has to distinguish between $t > 0$ and $t < 0$. Note that for $t < 0$ frustration can also appear in the hole motion. For example, a tight-binding particle on an isolated triangle gains a kinetic energy $|t|$ per particle, a factor of two smaller than for $t > 0$. Our results for a 32 cluster [22] are shown in Fig. 3 along the $\Gamma \leftrightarrow M$ line of the BZ [Fig. 1 (b)]. In all cases most of the spectral weight is found to be incoherent, distributed over a range of $7 - 9 |t|$. However, a small QP peak is visible, in particular for momenta close to the M -point. The region close to the Γ point has a tiny or no QP peak and the shape of the spectral function at Γ itself is very special, probably because of a higher point group symmetry. It is interesting to notice, in the case $t < 0$, the presence of a pseudo-gap in the region $\omega \sim 0$.

We have estimated the QP bandwidth W of the checkerboard lattice from the dispersion of its QP pole. As shown in the left panel of Fig. 4 the single hole bandwidth is much smaller than in a 2-leg spin ladder, which

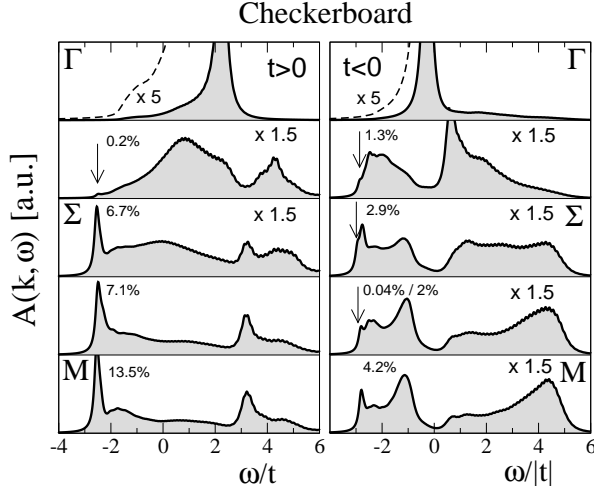


FIG. 3: Single hole spectral functions obtained on a 32 site checkerboard cluster along the line $\Gamma \leftrightarrow M$. Left panel $t = +1$, right panel $t = -1$. In both cases $J/|t| = 0.4$. When a quasiparticle peak is present the corresponding weight is indicated. Scaling factors are applied as indicated on the plots.

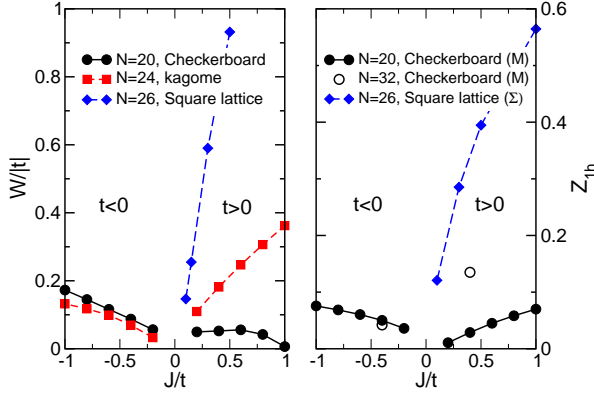


FIG. 4: Left panel: QP bandwidth in the checkerboard lattice vs J/t ($J > 0$). Comparison is shown with the case of the square lattice (data from Ref. [16]). The magnitude of the dispersion of the low-energy edge of the *kagomé* one-hole spectrum is also shown. Right panel: checkerboard QP weight at the M point of the BZ vs $J/|t|$ and square lattice QP weight at the $\Sigma = (\pi/2, \pi/2)$ point.

has a gapped spectrum, ($W \sim 2t$ for strong magnetic rung couplings [23]) or even in the square lattice, which has a gapless spectrum, where $W \sim 2.2J$. In the latter case, the strong renormalization of the coherent motion can be explained e.g. by long-wavelength spin-waves scattering [15, 16]. In the checkerboard lattice the QP are more massive, almost localized, although the VBC host has no low energy excitations. We believe that this remarkable fact is due to a destructive interference effect between the paths available for the hole to hop from one plaquette to the next. One can define QP weights $Z_{1h}(\mathbf{k})$ as the relative weights contained in the first δ -function appearing at the bottom of each spectrum in Fig. 3. Its behavior versus J/t is shown in the right panel of Fig. 4

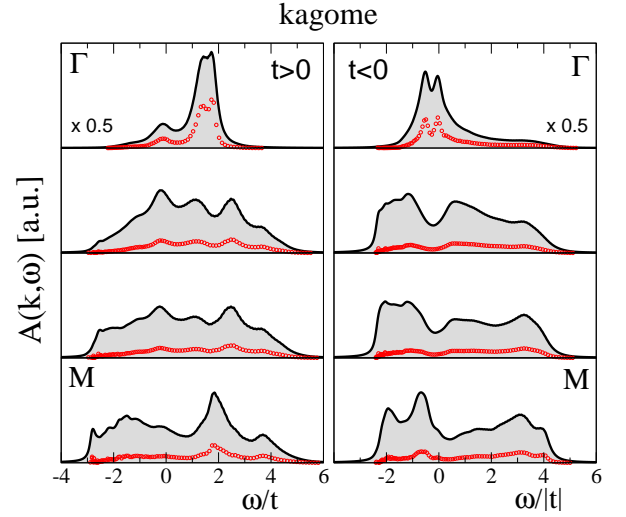


FIG. 5: Single hole spectral functions (black lines) along the line $\Gamma \leftrightarrow M$ computed on a 27 site *kagomé* cluster for $t = +1$ (left panel) and $t = -1$ (right panel). In both cases $J/|t| = 0.4$. The red circles denote pole locations and their residues. Note that no quasiparticle peaks are visible for all momenta.

and compared with existing data for the square lattice. We note that, although there are quantitative differences, the qualitative behavior is similar; larger J leads to larger holon-spinon confinement and hence to an increase of Z_{1h} .

The spectral functions of the *kagomé* lattice shown in Fig. 5 show exotic behaviors; they are very broad for all momenta (width $\sim 6 - 8 |t|$) and, in contrast to the checkerboard lattice, *do not show visible QP peaks* both for $t > 0$ (left panel) and $t < 0$ (right panel). Note that the broad appearance is not due to a large η , but is an intrinsic feature of the spectral function as can be seen from the large number of poles carrying spectral weight (circles in Fig. 5). Note that the GS $|\Psi_0\rangle$ of the 27 site undoped *kagomé* cluster is a spin $1/2$ state, e.g. $S^Z = +1/2$, $|\uparrow\rangle$. Therefore, the initial state of charge $Q = e$ and spin projection $S^Z = 0$, $c_{\mathbf{k},\uparrow}|\uparrow\rangle$, is an equal-weight superposition of a singlet and a triplet state leading to two contributions. We have checked that both components are consistent with the decay of the original hole into a holon and a spinon (with no QP peak). Close similarities of the singlet and triplet channels also suggest that the spinons in the final state (with either parallel or anti-parallel spins) are weakly interacting in agreement with the mechanism of spinon deconfinement.

The spectral function data strongly support a spin-charge separation scenario for the *kagomé* lattice. In order to get further evidence and more insight about the origin of this phenomenon we also investigate the spin density profile in the vicinity of the hole, i.e. the hole-spin correlation function $\langle n_i^h S_j^Z \rangle$ in the one hole-doped 30 site *kagomé* cluster (for which $S_Z = 1/2$). Results are shown in Fig. 6 for $t = +1$ (a) and $t = -1$ (b). In the case $t = +1$ we clearly see a repulsion between the net $S=1/2$

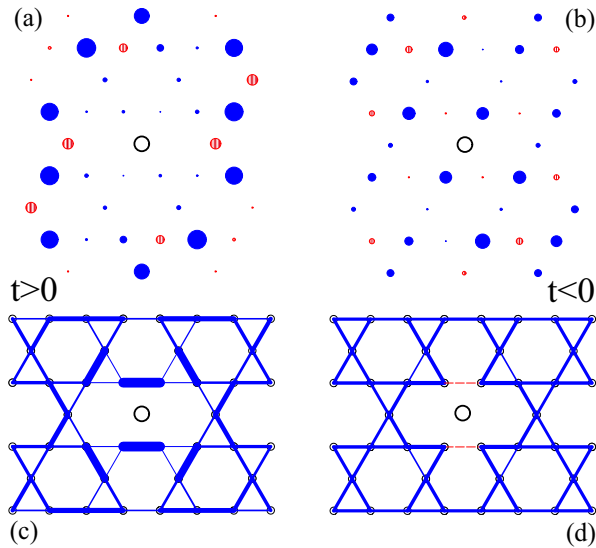


FIG. 6: (a-b) Hole-spin density-density correlation function $\langle n_i^h S_j^Z \rangle$ calculated on a 30 site *kagomé* cluster for both signs of t . The diameter is proportional to the magnitude of the correlation. Full blue (striped red) circles denote positive (negative) correlations. (c-d) Nearest neighbor bond spin-spin correlations around the mobile hole computed on a 27 site sample for both signs of t . $J = 0.4$ for all the plots. Full blue lines denote antiferromagnetic correlations, while the red, dashed lines stand for ferromagnetic correlations.

moment and the mobile hole. The case $t = -1$ displays a different picture, showing a rather uncorrelated behavior between the spinon and the holon. Nevertheless a spinon-holon confinement does not seem to be present, in agreement with spectral function data. In contrast we have checked that on a checkerboard lattice a clear localization of the spinon close to the holon takes place.

Finally we consider the GS of the one hole-doped 27 site *kagomé* cluster of total charge $Q = e$ and spin $S = 0$ to mimic the holon wavefunction. Figs. 6 (c,d) show a snapshot of the nearest neighbor spin correlations around the *mobile* holon. Surprisingly in the case $t = +1$ a “dimer freezing” is observed very similar to the *static* impurities considered in Ref. [21]. In contrast, the case $t = -1$ shows two slightly ferromagnetic bonds on the two triangles containing the holon, while the other bonds remain largely unaffected. This behavior of the magnetic environment is fairly well described by a simple energetic consideration on a 3-site ring $t-J$ model; for $t = +1$ the propagating holon is accompanied by a singlet, while in the opposite $t = -1$ case an accompanying ferromagnetic bond appears.

To conclude, based on extensive analysis of the single particle spectral functions and various charge-spin correlations in the single hole GS, we have addressed the issue of spin-charge separation in 2D magnetically disordered magnets. We show strong evidence that it occurs in the *kagomé* lattice and we expect it to be robust for small but

finite doping. This provides the first example of observed spin-charge separation in a two-dimensional microscopic model. The RVB nature of the undoped groundstate (characterized by a gapless low-excitation singlet spectrum) seems to be crucial for this behavior. Indeed, in the checkerboard lattice, which exhibits a VBC structure, a weak hole-spinon confinement manifests itself as QP peaks for some momenta.

We thank M. Mambrini for useful discussions. A.L. acknowledges support from the Swiss National Fund and the CNRS. D.P. thanks the Institute for Theoretical Physics, ETH Zürich, for hospitality during the final stage of this work. We thank IDRIS (Orsay) and the LRZ München for allocation of CPU-time.

-
- [1] P.W. Anderson, Science **235**, 1196 (1987); P.W. Anderson *et al.*, Phys. Rev. Lett. **58**, 2790 (1987).
 - [2] N. Read and S. Sachdev, Phys. Rev. Lett. **62**, 1694 (1989).
 - [3] R. Moessner *et al.*, cond-mat/0106286; B. Canals, Phys. Rev. B **65**, 184408 (2002).
 - [4] J.-B. Fouet *et al.*, Phys. Rev. B **67**, 054411 (2003).
 - [5] W. Brenig and A. Honecker, Phys. Rev. B **65**, 140407(R) (2002).
 - [6] V. Elser, Phys. Rev. Lett. **62**, 2405 (1989); P.W. Leung and V. Elser, Phys. Rev. B **47**, 5459 (1993); J.T. Chalker and J.F.G. Eastmond, Phys. Rev. B **46**, 14201 (1992).
 - [7] P. Lecheminant *et al.*, Phys. Rev. B **56**, 2521 (1997); C. Waldtmann *et al.*, Eur. Phys. J. B **2**, 501 (1998).
 - [8] N. Read and S. Sachdev, Phys. Rev. Lett. **66**, 1773 (1991); A.A. Nersisyan, A.M. Tsvelik, Phys. Rev. B **67**, 024422 (2003).
 - [9] P. Mendels *et al.*, Phys. Rev. Lett. **85**, 3496 (2000); L. Limot *et al.*, Phys. Rev. B **65**, 144447 (2002).
 - [10] A.P. Ramirez *et al.*, Phys. Rev. Lett. **89**, 067202 (2002); I. Mirebeau *et al.*, Nature (London) **420**, 54 (2002).
 - [11] K. Takada *et al.*, Nature (London) **422**, 53 (2003).
 - [12] G. Baskaran, Phys. Rev. Lett. **91**, 097003 (2003); see also G. Baskaran *et al.*, Solid State Commun. **63**, 973 (1987).
 - [13] P.W. Anderson, Phys. Rev. Lett. **64**, 1839 (1990).
 - [14] W.F. Brinkman and T.M. Rice, Phys. Rev. B **2**, 1324 (1970).
 - [15] S.A. Trugman, Phys. Rev. B **37**, 1597 (1988).
 - [16] P. Bérán, D. Poilblanc and R.B. Laughlin, Nucl. Phys. B **473**, 707 (1996) and references therein; M. Brunner *et al.*, Phys. Rev. B **62**, 15480 (2000).
 - [17] For ARPES studies on the 2D AF insulator $\text{Sr}_2\text{CuO}_2\text{Cl}_2$ see C. Kim *et al.*, Phys. Rev. Lett. **80**, 4245 (1998).
 - [18] The J_1 - J_2 square lattice model might exhibit a similar VBC GS with columnar dimer order and a smaller spin gap; see H.J. Schulz, T. Ziman and D. Poilblanc, J. Phys. I (France) **6**, 675 (1996) and references therein.
 - [19] E. Berg *et al.*, Phys. Rev. Lett. **90**, 147204 (2003).
 - [20] F. Mila, Phys. Rev. Lett. **81**, 2356 (1998); see also V. Subrahmanyam, Phys. Rev. B **52**, 1133 (1995).
 - [21] S. Dommange *et al.*, Phys. Rev. B **68**, 224416 (2003).
 - [22] We use the cluster 32^* as defined in Ref. [4].
 - [23] See e.g. M. Troyer *et al.*, Phys. Rev. B **53**, 251 (1996).